Sensors for Hydrogen Peroxide Detection

Subjects: Chemistry, Analytical | Engineering, Biomedical
Contributor: Vinay Patel

Hydrogen peroxide (H2O2) is a key molecule in numerous physiological, industrial, and environmental processes. H2O2 is monitored using various methods like colorimetry, luminescence, fluorescence, and electrochemical methods. Here, we aim to provide a comprehensive review of solid state sensors to monitor H2O2. The review covers three categories of sensors: chemiresistive, conductometric, and field effect transistors. A brief description of the sensing mechanisms of these sensors has been provided. All three sensor types are evaluated based on the sensing parameters like sensitivity, limit of detection, measuring range and response time. We highlight those sensors which have advanced the field by using innovative materials or sensor fabrication techniques. Finally, we discuss the limitations of current solid state sensors and the future directions for research and development in this exciting area.

Keywords: solid state sensors ; field effect transistor ; chemiresisitive sensor ; conductometric sensor ; hydrogen peroxide ; biosensor and sensors

1. Introduction

H_2O_2 plays an important role in various applications such as medical diagnostics, clinical research, and industrial sectors like food processing, paper, textile, pharmaceuticals as well as cleaning and disinfection products (Figure 1) [1]. H_2O_2 is also important physiologically and is involved in metabolic activities, apoptosis, and immune cell activation [2][3]. It plays an important role as an oxidative stress marker, defense agent, and aging [2][4]. It is a crucial biomarker in monitoring various diseases and disorders including diabetes [5], cancer [6], Parkinson's [7], cardiovascular, Alzheimer's [7], and neurodegenerative disorders [7][8]. Moreover, H_2O_2 is the intermediate molecule formed in reactions involving numerous oxidases such as glucose oxidase, alcohol oxidase, cholesterol oxidase, lactate oxidase, and glutamate oxidase [9]. Further, H_2O_2 is used for sterilizing various medical equipment and residual H_2O_2 levels need to be monitored to ensure that the equipment is safe to use [10].

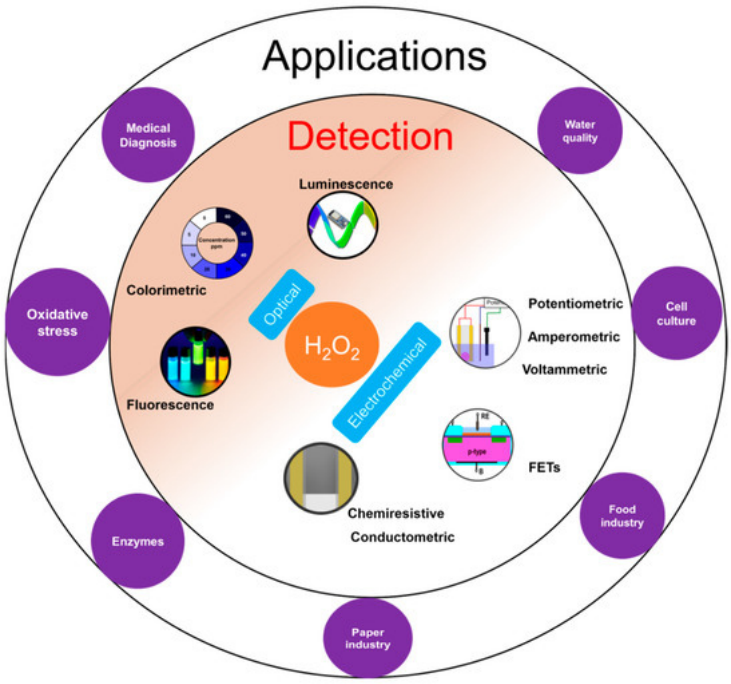

Figure 1. Overview of H_2O_2 detection with inner circle containing the two common detection principles: optical and electrochemical; and outer circle with few applications areas of H_2O_2 detection.

H_2O_2 measurement and quantification is performed in a variety of sample matrices including environmental samples like water and soil, human fluids like sweat, blood, cell and tissue cultures. H_2O_2 is measured using diverse range of methods such as optical [11][12] including colorimetry, chemiluminescence, and fluorescence; and electrochemical [13][14][15][16] including potentiometry, voltammetry and amperometry (Figure 1). Optical techniques are limited by high cost, complex testing processes, the requirement of sophisticated and bulky instrumentation, need for trained personnel to operate, and interference from sample matrices. On the other hand, electrochemical sensors offer low-cost, simple

instrumentation and fast detection [13]. Nevertheless, electrochemical sensors also suffer from a few limitations such as the requirement for a reference electrode, larger working area, etc. The potentiometric method requires a reference electrode for reliable potential measurement while amperometric sensors require a reference electrode to apply a reliable potential bias for the measurement. For potentiometric sensors, a stable response strongly depends on the stability of the reference electrode. However, a miniaturized solid-state reference electrode with long term stability is yet to be realized [17]. For amperometric sensors, a high working electrode potential results in increased interference from interfering molecules [18].

More recently, solid-state sensors such as chemiresistors [19][20][21], conductometric sensors [21][22][23] and field effect transistors (FET) [24][25][26] have been used to measure H_2O_2 while avoiding the aforementioned challenges. Chemiresistors consist of a single sensing layer which measures the change in analyte concentration through alteration in resistance of the layer using two contact electrodes. A small potential bias is applied to the substrate film and the change in current is measured. Advantages of chemiresistors are: high sensitivity, because the resistance changes can occur due to modification at any position of the network unlike techniques like colorimetric which is based on volume modifications; ease of fabrication of sensor arrays due to simple sensor structure; suitability for miniaturization; simple instrumentation setup for measurement and elimination of the need for reference electrodes unlike electrochemical methods [27]. FET based solid state sensors are attractive due to their ability to detect analytes with ultrahigh sensitivity. In addition, FETs can be manufactured easily using the established manufacturing process for metal oxide semiconductor FETs (MOSFET) [9].

Previous reviews on sensors for H_2O_2 detection have typically focused on electrochemical and colorimetric sensors. Several papers have been published on enzymatic [1][13][14][16][28][29] and non-enzymatic sensing [1][15][30][31] using those principles and the readers are referred to them for an in-depth analysis in these areas. An in-depth review of the emerging class of solid state H_2O_2 sensors is not currently available. This review is focused exclusively on chemiresistive, conductometric and FET based H_2O_2 sensors which have significant potential for field deployment. A critical analysis of the sensing methods with emphasis on the sensing mechanisms and important parameters like measuring range, limit of detection (LOD), and response time have been provided. The diverse range of functional materials used for sensing and to fabricate these sensors have also been discussed.

2. Sensing Mechanism

2.1. Chemiresistive Sensors

Chemiresistive sensors are a group of sensors which transduces the chemical changes to resistance change. The sensor response is attributed to surface reactions or adsorption of analyte molecules on the sensing film [32]. This type of sensor was originally developed for gas sensing by monitoring resistance changes with adsorption of gas molecules on the sensor surfaces [32][33]. Typically, a sensor is placed under a small potential bias and the change in current is measured as output and converted into a change in resistance. A general chemiresistor consists of four components: the sensitive or active thin film substrate, contact electrodes, passivation layer and substrate (Figure 2a,b). Although for gas sensing, the contacts may be exposed to the environment, they are typically covered with an insulating film to avoid electrical shorting, especially when used in conducting liquids. The equivalent electrical circuit for a chemiresistive sensor can be represented as shown in Figure 2c, where both contacts are represented by parallel RC circuit depicting both Faradaic and non-Faradaic processes. The sensing layer which remains in contact with the solution is divided into three parallel RC circuits representing surface, bulk, and interface processes. When chemiresistive sensors are operated in DC mode, all capacitance can be neglected from the equivalent circuit (Figure 2c).

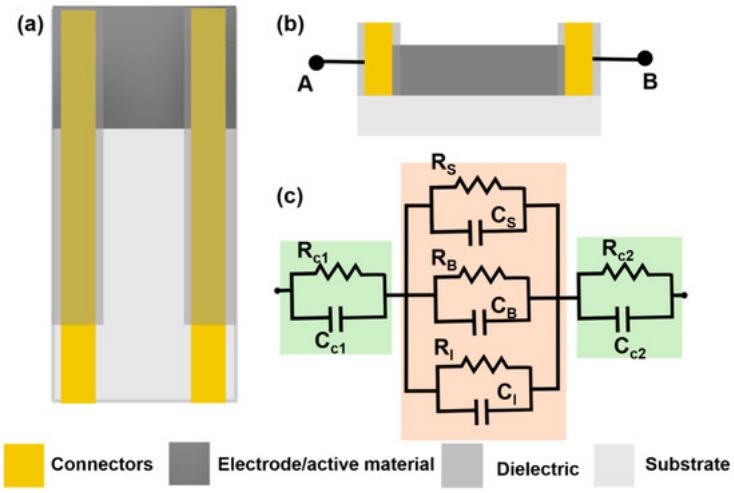

Figure 2. (**a**) Top view of a chemiresistive sensor with 4 main components: active material (dark grey), connectors or contacts (gold), dielectric to insulate the contacts (grey) and substrate (light grey) (**b**) A transverse section of a chemiresistive sensor with two connecting outputs (**c**) An electrical circuit analog for the chemiresistive sensor with R_{c1}

and R_{c2}, the contact resistance for the first and second contacts, while R_S, R_B and R_I are the solution, bulk and interfacial resistance. Similar to resistance, capacitance of all the surfaces are labelled accordingly.

During measurement, the sensor is exposed to the analyte, and adsorption of analyte to the active thin film results in a change in resistance. For instance, carbon nanotubes (CNTs) are generally p-doped when the films are coated using water based CNT dispersions and if analyte adsorption results in the release of electrons, the hole concentration in the active surface is reduced, which results in a decrease in resistance [34]. On the other hand, if the analyte extracts electrons from the CNT film, this will lead to an increase in dominant carriers resulting in an increase in conductivity. Further, this change in resistance due to analyte interactions can occur from factors like increasing the CNT-CNT junction resistance modulation of the Schottky barrier at the CNT-metal contact junction and charge transfer between analyte and CNT. These processes have been described in detail in other reviews [35][36]. These sensors have some limitations such as irreversible changes introduced onto the substrate due to application of a potential bias, a high dependence of the sensitivity of the sensor on the substrate thickness, and high contact resistance which can further reduce the sensitivity of the sensor. For instance, in the case when conducting polymers are used as the functional sensing layer, the potential bias can induce an irreversible change in the polymer film resulting in a change to the baseline resistance of the sensor. The analyte can also cause irreversible changes to the sensors surface [19]. Thinner films generally have higher sensitivity as compared to thicker films [33]. For two point measurements, the resistance change has two components: change due to the analyte binding and change in contact resistance between the substrate and the metal contacts [37].

2.2. Conductometric Sensors

Conductometric sensors are devices which detect the change in conductivity of the analyte solution due to consumption or generation of ions due to chemical reactions using two conducting electrodes [38]. This method was originally developed to study chemical kinetics of reactions and later exploited by researchers to detect enzyme catalyzed reactions. Conductometric measurements are non-specific as conductivity changes can occur due to the migration of all ions present in the solution. This non-specificity is circumvented by coating enzyme on top of the electrode and doing the measurements in a defined measuring cell. Conventionally, the conductivity measurements are performed in AC mode. Unlike chemiresistive sensors, these sensors offer information through the frequency of the measurement, an important experimental variable to determine non-Faradaic processes. An alternating bias has several advantages such as minimized contact polarization, double layer charging and electrode polarization [39].

Typically, conductometric measurements are done using a pair of identical electrodes (generally interdigitated electrodes) dipped in a solution container with a constant volume. One of the interdigitated electrodes (IDE-1) is coated with the enzyme film and the other does not have any enzyme layer (IDE-2) (Figure 3a). The IDE-2 determines the base conductivity response from other ions and molecules present in the solution. The measurement of both the sensors are done with respect to a counter and/or reference electrode (Figure 3b). The final sensor response is determined by subtracting the signal of IDE-1 from the signal of IDE-2. Here, the impedance is measured perpendicular to the electrode surface. The equivalent circuit of the electrochemical cell is shown in Figure 3c where R_{ct1} and R_{ct2} are the charge transfer resistances for IDE and CE respectively, W is the Warburg impedance for the IDE which models the diffusional resistance due to both interfaces, C_{dl1} and C_{dl2} are double layer capacitances of IDE and CE respectively and R_s is the solution resistance. Enzymatic conductometric sensors are versatile sensors which are low-cost, need a smaller potential bias and require simple instrumentation to generate reliable signals. However, the sensing signal can be affected by temperature variations [39] and changes in the ionic strength of the solution.

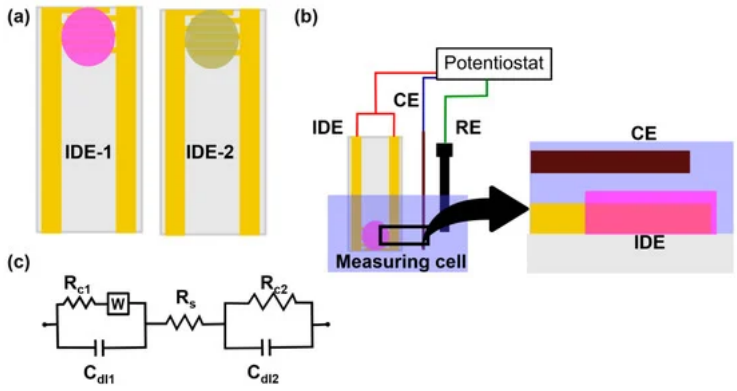

Figure 3. (**a**) A pair of interdigitated electrodes (IDE): IDE-1 represents the active membrane coated electrode and IDE-2 is the electrode coated with membrane without any active material (**b**) A schematic representing the experimental setup of a conductometric sensor with IDE, a counter electrode and a reference electrode. The zoomed in picture shows a transverse section of IDE and counter electrode (**c**) An equivalent circuit for the conductometric sensor with R_{C1}, W and C_{dl1} representing the charge transfer resistance, Warburg impedance and double layer capacitance, respectively for the IDE; R_S is the solution resistance; and R_{C2} and C_{dl2} representing the charge transfer resistance and double layer capacitance for the counter electrode respectively.

2.3. FET

Metal oxide field effect transistors (MOSFETs) are used in electronic circuits as switches, gates, amplifiers etc. MOSFETs can be three or four terminals depending on the presence or absence of back gate (base substrate): source, drain, gate and base substrate. Insulated gate FET (IGFET) is the most common type of MOSFET used currently for chemical sensing. The gate terminal of the IGFET is insulated using a dielectric layer (like SiO_2). A typical n-channel FET is constructed using a p-type substrate with heavily doped n-type source and drain (Figure 4a). The operation of the FET depends on the potential bias applied to the gate. Under zero bias, the FET channel is non-conducting. For n-channel FET, the conduction begins after a critical threshold potential is applied to the gate. This threshold potential will induce an inversion layer.

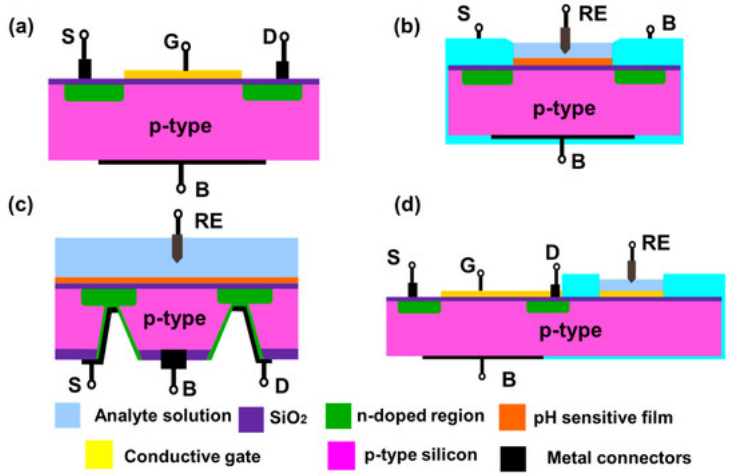

Figure 4. Schematics of a (**a**) MOSFET with p-type silicon as a base substrate (pink) and n-doped source and drain region (green) (**b**) ISFET with a pH sensitive film (orange) (**c**) Back gated FET with analyte solution and RE on the top side and all the terminal connections are done from the back side (**d**) Extended gate FET with a regular MOSFET and an extended sensing region connected with gate terminal of the MOSFET. S, G, D and B are source, drain, gate and base substrate terminals (all shown in black). RE is the reference electrode.

Early H_2O_2 (and glucose) FET sensors had pH sensitive material coated on the gate insulator that made it sensitive to changes in local pH due to generation or consumption of hydrogen ions by an enzyme that catalyzes H_2O_2 (Reaction 1) [40][41][42]. In this reaction, the reduction of H_2O_2 was catalyzed in presence of horseradish peroxidase (HRP), with the iodide ion acting as a reducing agent [43].

$$H_2O_2 + 2I^- + 2H^+ \xrightarrow{HRP} I_2 + 2H_2O \quad (1)$$

In such FETs, the gate dielectric is converted into a hydrogen sensitive film which can generate similar potential change in presence of the analyte (Figure 4b). Then the channel conduction can be influenced by changes in the hydrogen ion concentration. These devices are known as ion selective FETs (ISFETs). Similar to MOSFETs, ISFETs can also be n-channel or p-channel ISFET depending on the doping of the silicon substrate used to fabricate the FET. The drain current depends on the resistance of inversion layer and, the potential applied between source and drain. Mathematically, the drain current (I_d) of ISFET is given by [9]:

$$I_d = \mu C_i \left(\frac{W}{L}\right) V_d \left[V_g - \left(E_{ref} - \phi + \chi_{sol} - \left(\frac{\phi_{Si}}{q}\right) - \frac{Q_i + Q_{ss}}{C_i} - \left(\frac{Q_b}{C_i}\right) + 2\phi_f\right) - 0.5V_{ds}\right] \quad (2)$$

where μ is mobility of electrons in the channel; L and W are length and width of the channel, respectively; q is the elementary charge, Q_b, Q_i, Q_{ss} are the charges located in depletion region, insulator region, and surface and interface states, respectively, χ_{sol} is solution's surface dipole potential, E_{ref} is the reference electrode's potential, ϕ_{Si} is the electron work function of silicon, ϕ_f is the potential difference between Fermi level of doped and intrinsic silicon, V_{ds} is the potential applied to the drain with respect to source, V_d is the drain potential, V_g is gate potential, C_i is the capacitance value of the gate, and ϕ is the potential of membrane–electrolyte interface.

Commonly used pH sensitive materials for ISFETs are silicon nitride (Si_3N_4), aluminum oxide (Al_2O_3), and tantalum oxide (Ta_2O_5) [9][40][41][42][43][44][45][46]. pH sensitivity is a surface phenomenon where the surface hydroxyl groups interact with the protons. The consequent changes in the surface charge or potential of the gate material leads to a current flow in the channel. This generated current is proportional to the analyte concentration. ISFETs are increasingly popular due to advantages such as rapid detection, small size, established manufacturing process, easy integrability in arrays, and their ability to be stored in dry form. However, they suffer from higher drift as compared to ion selective electrodes.

Based on its design, the ISFETs can be front side and back side connected. Front side ISFETs are widely used due to ease of fabrication, but they make it difficult to passivate the device from the analyte solution. Back side ISFETs solve the passivation problem as all the connections are accessed from the back side of the silicon chip. However, it poses a manufacturing difficulty to etch a deeper cavity into the silicon chip for connecting the source and drain from the back side of the chip (Figure 4c). An alternate configuration known as an extended gate FET was proposed in 1983 [47] (Figure 4d). The device has two components: a MOSFET with electrical connections and an extended gate with a pH sensitive film. This device has advantages such as low manufacturing cost due to simpler fabrication and packaging, and long term environmental stability of the device as the FET is not directly exposed to the solution.

3. Chemiresistive Sensors

Chemiresistive sensors were initially developed to detect gases or vapors but in the past two decades several chemiresistive sensors have also been developed to measure analytes in liquid environments. These sensors consist of two main components: an active thin film and electrical contacts. One of the first H_2O_2 chemiresistive sensor was fabricated from polypyrrole and multiwalled CNT (MWCNT) [48]. Chemiresistive sensors can be broadly classified based on active sensing thin film material. The active thin film can be made of various conducting or semiconducting materials such as CNTs [19][48][49], conducting polymers [20][50][51] or combinations of these materials. Contact electrodes are made of conductive materials including conductive carbon [50][51], metal electrodes like platinum [48], gold [19][20][52], and silver [49]. The sensors are compared based on three parameters: measuring range, LOD and response time. A summary of H_2O_2 chemiresistive sensors is given in Table 1.

Table 1. A list of H_2O_2 chemiresistive sensors with the crucial sensor properties including LOD, measuring range, voltage bias, response time, buffer and working pH. All units are as mentioned in the top row unless specified. Where NR: Not reported, PPy: Polypyrrole, PANI: Polyaniline, Pt NPs: Platinum nanoparticles, SnO_2: Tin oxide, Au: Gold.

Substrate	Target analyte	Ligand/ Enzyme	LOD (mM)	Measuring range (mM)	Voltage bias (mV)	Response time (s)	Buffer/working pH	Comments	Interference tested	Ref
Carbon nanotube based										
PPy-MWCNT	H_2O_2/ Glucose	Dodecyl benzene sulfonate	NR	0–20	1	NR	NR	Investigated the sensitivity of temperature humidity etc.	No	[48]
CNT	Glucose	EGCG-GOD	8.7 nM	10 nM–1 µM	100	<400 (est.)	Working pH 7.4 Buffer: PBS	Sensor responds to all reactive oxidative species	Yes	[49]
SWCNT-PVP	Glucose	GOD	0.08	0.02–2	100	3	Working pH 5.5 Buffer: Acetate	Tested in juice & iced tea Stable for 5 consecutive tests	Yes	[19]
Conducting polymer based										
Au-PANI nanowires	H_2O_2	AgNPs	5	5–40	20	25	Working pH 5 Buffer: Phosphate (200 mM)	Stable response for 36 h Reusable sensor	Yes	[20]

MWCNT-PANI nanowires	H_2O_2	AgNPs	1	1–20	NR	180	NR	Inkjet printed sensors	No	[51]
MWCNT-PANI nanowire	H_2O_2 Glucose	PtNPs	2	2–10	500	240	NR	Inkjet printed	No	[50]
Others										
Alumina	Glucose	SnO_2-GOD	0.5 (est.)	0.5–20	NR	50	Working pH 7.2 Buffer: Phosphate	Sensor sensitivity increases with deposition temperature of SnO_2	No	[53]

4. Conductometric Sensors

One of the earliest conductometric sensors for H_2O_2 was developed in 1999 [43]. The sensor was constructed using tetra-tert-butyl copper phthalocyanine (ttb-CuPc) coated gold interdigitated electrodes on a ceramic substrate (Figure 5a). The phthalocyanine film was deposited using the Langmuir-Blodgett method. The sensing of H_2O_2 was based on oxidation of iodide ions by H_2O_2 in the presence of HRP (Reaction 1). The iodine concentration was measured by a conductometric sensor based on ttb-CuPc as the sensing layer. The effect of other interfering species in the sample was suppressed using a hydrophobic gas permeable membrane. HRP was immobilized on top of the gas permeable membrane. The sensor attained a steady state response in ~10 min which was due to slow conductivity changes in the phthalocyanine film. The highest sensor response was obtained within a pH range of 5.0–6.5. The measuring range was 0.005 to 0.3 mM with a sensitivity of 0.042 µS/µM of H_2O_2. The sensor worked continuously for 7 h with more than 30 measurements and had a storage stability of 90 days when stored at 4 °C.

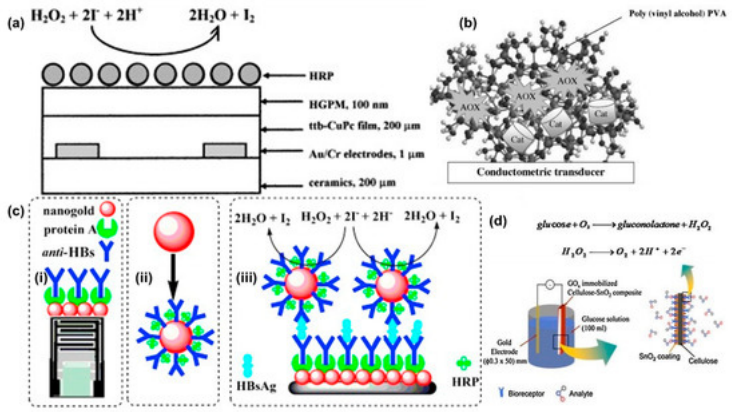

Figure 5. (**a**) A HRP conductometric sensor for enzymatic detection of H_2O_2. The sensor was fabricated using HRP as the enzyme and ttb-CUPc as the active/sensitive film to detect the released iodine molecule. Reprinted from [38] with permission from Elsevier. (**b**) A bi-enzyme sensor (Alcohol oxidase and catalase) to detect alcohol using conductometric transducer. Reprinted from [39] with permission from Elsevier. (**c**) (**i**) Schematics of a conductometric transducer working as an immunosensor (**ii**) A nanogold particle coated with anti-HBs and protein A (**iii**) Schematics of the sandwich immunoassay with the reactions involved to measure Hepatitis-B surface antigens. Reprinted from [42] with permission from Elsevier. (**d**) Schematics of a GOD immobilized cellulose-SnO_2 composite electrode. Reprinted from [46] with permission from Elsevier.

Since then, multiple conductometric sensors have been reported in the literature. These sensors can be classified based on electrode material used for the sensors such as metal [43][54][55][56], metal nanoparticles [21][22][23][57], and others [58]. The sensors are compared based on crucial parameters like sensitivity, measuring range, LOD, potential bias, and response time. A summary of conductometric sensors is given in Table 2.

Table 2. Summary of H_2O_2 conductometric sensors with the crucial sensor properties including LOD, measuring range, voltage bias, response time, buffer and working pH. Where AOX: Alcohol oxidase, PVA: Polyvinyl alcohol, g-C_3N_4: graphitic carbon nitride, Au: Gold, AuNPs: Gold nanoparticles, AFP: alpha-fetoprotein, LOD: Lactate oxidase.

Substrate	Target Analyte	Ligand/ Enzyme	LOD (μM)	Measuring Range (mM)	Voltage Bias (mV) (Frequency)	Response Time (Minutes)	Buffer/Working pH	Comments	Interfer Tested
Metal interdigitated electrodes									
Ceramic-Au	H_2O_2	Pthalocyanine	NR	0.005–0.3	60	10	Working pH 6.0 Buffer: Phosphate (20 mM)	Storage stability for 90 days at 4 °C	No
Silicon-Au	H_2O_2/ Cyanide	PVA-Catalase	6	0–100	10 (100 kHz)	5	Working pH 7.2 Buffer: Phosphate (5 mM)	Inhibitory assay for cyanide detection	No
Au	Methanol Ethanol Propanol	AOX-Catalase	0.5 1 3	<0.075 <0.070 <0.065	10 (100 kHz)	<10	Working pH 7.2 Buffer: Phosphate (5 mM)	Alcoholic beverages	Yes
Ceramic-Au	Lactate	LOD-HRP	0.05	0–0.21	10 (100 kHz)	~20 (est.)	Working pH 6 Buffer: Phosphate (5 mM)	Diluted yogurt samples Storage stability for 40 days at 4 °C	Yes
Metal nanoparticles									
AuNPs	Hepatitis B (HB)	HRP/Anti-HBs	0.01 ng/mL	0.1–600 ng/mL	10 (100 kHz)	>30	Working pH 7.0 Buffer: Phosphate (10 mM)	Tested with serum samples Assay stable for 16 days when stored at 4 °C	Yes
Ceramic-Au & magnetic NPs	Glucose	GOD	3	0.04–3	10 (100 kHz)	<10	Working pH 7.3 Buffer: Phosphate (5 mM)	Stable for 12 days when stored at 4 °C	No
g-C_3N_4	AFP/H_2O_2	Pt NPs	0.01 ng/mL	0.01–100 ng/mL	10 (100 kHz)	5–6	Working pH 6.5 Buffer: PBS (10 mM)	Tested with human serum Inhibitory Immunoassay	Yes
Others									

Cellulose-SnO_2	H_2O_2/ Glucose	GOD	500	0.5–12	0–3 V (dc)	NR	Working pH 7.2 Buffer: Phosphate	Storage stability > 10 days Flexible one-time use sensor	No

5. FET Sensors

H_2O_2 is not an ideal molecule to detect using electrochemical reactions due to its slow reaction kinetics. Amperometric sensors overcome this by applying a suitable potential to accelerate the reaction kinetics. However, this overpotential limits the detection at low concentrations because of a high signal to noise ratio. Similar detection limit issues exist for potentiometric sensors. In FET sensors, the phenomenon of surface charging at the gate and the effect of it on the inversion layer created and the conductivity of the channel is non-linear and hence the amplification can result. FET sensors can be classified in to four major groups based on the active material used for the detection: silicon nitride [40][41][42][45][46][59][60][61], conducting polymers [62][63][64][65][66], metal oxide [44][67][68][69][70][71][72][73], and carbon nanomaterials [24][25][74][75][76][77][78]. The sensors are evaluated based on crucial parameters like measuring range, sensitivity, detection limit, and response time. FET sensors are summarized in Table 3.

Table 3. Summary of various FETs used for H_2O_2 measurement where OC: operating conditions; PANI: Polyaniline; PAA: poly acrylic acid; pDAB: poly(1,2 diaminobenzene); HRP: Horseradish peroxidase; PVP: poly(4-vinylpyridine-co-styrene); MOSC: Metal oxide semiconductor capacitor; 3-aminopropyltriethoxysilane (APTES), PPyNT: Polypyrrole nanotube, Pt: Platinum, I_s: source current, V_{ds}: Drain potential with respect to source, V_g: is gate voltage, I_{ds}: current between drain and source, V_d: Drain potential, V_{bias}: potential bias applied between the Pt electrode and reference electrode, I_{bias}: current bias, pDAB: poly(1,2-diaminoben-zene), ITO: Indium titanium oxide, GluD: Glutamate dehydrogenase, UA: Uric acid, AA: Ascorbic acid and MoS_2: Molybdenum disulphide.

Substrate	Target Analyte	Ligand/ Enzyme	LOD (μM)	Sensitivity	Measuring Range (mM)	OC	Response Time (s)	Working pH & Buffer	Comments
Silicon nitride FET									
Si_3N_4-FET	H_2O_2	HRP	5	~15 mV/mM (est.)	<2	I_s: 300 μA V_{ds}: 2 V	30–90	Buffer: Phosphate (10 mM) Working pH: 6	<10% reduction enzyme activity a 1000 measureme
Si_3N_4-FET/Pt electrode	Glucose	GOD	NR	~40 mV/mM	<5	V_{bias}: 0.64 V	~480	Buffer: Phosphate (5–20 mM) Working pH: 7.4	Baseline establis by removing potential bias
Si_3N_4-FET/Pt electrode	Glucose & sucrose	GOD & Invertase-mutarotase-GOD	~50 (est)	NR	1.67–16.67	V_{bias}: 0.7 V	180–300	Buffer: Phosphate (10 mM) Working pH: 7.4	Greater Pt a increases sensitiv

Si_3N_4-FET/Pt electrode	Glucose	GOD	1000 (est.)	~11 mV/mM (est.)	1–10	V_{bias}: 0.7 V	~60	Buffer: Phosphate (10 mM) Working pH: 7.4	Ladder shape electrode was u for potential bias
Si_3N_4-FET	H_2O_2	Pt	10000	5 mV/mM	10–100	I_{ds}: 0.1 mA V_{ds}: IV	300	Buffer: Phosphate (100 mM) Working pH: 7.2	Used for glucose lactate
Conducting polymers									
Carbon	H_2O_2	PANI-pDAB-HRP	100	NR	<0.5	V_g: 200 mV V_d: 20 mV	~100 s	Buffer: citrate-phosphate-Na_2SO_4 Working pH: 5	HRP inhibition H_2O_2 concentra > 0.5 mM.
Kapton-Carbon	H_2O_2	PSPANI-HRP	25	0.126 µA/s	0.025–1	V_g: 0 V V_d: 20 mV	100–300 s	Buffer: HEPES-KNO_3 (100 mM) Working pH: 7	Sultonation impro the PANI conduct at pH 7
Si_3N_4-FET	Glucose	PANI-PAA-GOD	NR	1 nA/mM	0–9	V_g: 20 mV V_{ds}: 10 mV	<1 s	Buffer: McIlvaine Working pH: 5	PANI-PAA film deposition electropolymeriza
PEDOT-TFT	H_2O_2 & Glucose	GOD	100	NR	0.1–1	V_d: 0.2 V V_g: 0–0.6 V	~60 s	Buffer: PBS Working pH: 7.14	pH indepen response from p to 9
PEDOT-TFT	Glucose	GOD	1	0.1 V/decade	<1	V_{ds}: −0.2 V	NR	Buffer: PBS (15 mM) Working pH: 6.8	Sensitivity can improved increasing Vg
PEDOT-TFT	Glucose	GOD	<1000	1.65 µA/mM	1.1 to 16.5	V_{ds}: −1.5 V V_g: 0.0 V	10–20 s	NR	Sensor encapsulated cellulose ace membrane

Liquid gate-FET	H_2O_2 & Glucose	PPyNT-GOD	500 (est.)	3.75%/mM (est.)	2–20	V_{ds}: −0.01 V V_g: 0.01 V	5–10 s	Buffer: PBS (10 mM) Working pH: 7.0	High enzyme loa was achieved
TFT	H_2O_2 & Glucose	PEDOT-GOD	1	0.79–3 µA/mM	0.001–5	V_{ds}: −0.4 V V_g: 0.4 V	<20 s	Buffer: PBS Working pH: 7.4	Used as both op and electrochemi
TFT	Glucose	PEDOT-GOD	10	NR	0.01–100	V_{ds}: −0.7 V V_g: 0.7 V	~360 s	Buffer: PBS (120 mM)	Stable for 100 c with covale immobilized GOD
TFT	H_2O_2 & Glucose	PEDOT-TiO_2-GOD	1	0.126%/decade	0.001–5	V_{ds}: −0.1 V V_g: 0.4 V	~1000 s (est.)	Buffer: PBS (10 mM) Working pH: 7.0	Stable for 10 c with intermit testing
Liquid gate FET	H_2O_2	rGO-PPy NTs	0.1 nM	2%/decade	0.1–100 nM	V_g: 0.1 V V_{ds}: −0.01 V	<1 s	Buffer: PBS Working pH: 7.4	Stable up to month, when st in air
Metal oxides									
Glass-ITO-SnO_2	Glucose	GOD-MnO_2	2700	2.35 mV/mM	<20	No bias	720	Buffer: Phosphate-KOH (5 mM) Working pH: 8.1	Dynamic ra strongly depends pH value
Si_3N_4-FET	Glucose	GOD-MnO_2 NPs	20	NR	0.025–1.9	No bias	~140 s	Buffer: Tris (10 mM) Working pH: 7.4	Repeatability: 1 (RSD) for measurements
		Iridium oxide	100	400 mV/dec	0.1–10	I_{bias}: 25 nA		Working pH: 3.5–9	
FET	H_2O_2	Prussian blue	10	290 mV/dec	0.01–1	I_{bias}: 50 nA	NR	Working pH: 4.5–6	-
		Os-PVP-HRP	0.1	700 mV/dec	10^{-7}–10^{-5} M	I_{bias}: 25 nA		Working pH: 4.5–6	

Ta_2O_5-FET-Pt	H_2O_2	Perovskite oxide	4	35 mV/dec	0.005–0.2	I_{bias}: 25 nA	1800	Buffer: Phosphate Working pH: 7	Change stoichiometry oxide can resul lower detection li
FET	H_2O_2	TiO_2	NR	4.5 mV/μM (DMEM media)	NR	I_{ds}: 0.1 mA V_{ds}: 1 V	300 (est.)	Buffer: Phosphate	DMEM media
FET	Glucose	ZnO-NiO quantum dots	26	13.14 μA mM^{-1}(0.001–10 mM)	0.001–50	V_g: 1.2–2 V V_{ds}: 0.0 V	NR	Buffer: PBS (10 mM) Working pH: 7.4	Tested in w blood and serum
Liquid gate FET	Glucose	ZnO rod-GOD	0.07	32.27 μA $mM^{-1}cm^{-2}$	0.05–70	V_g: 0–2 V	NR	Buffer: PBS (50 mM) Working pH: 7.4	Mice blood, serur
	Cholesterol	ZnO rod-COD	0.04	17.1 μA $mM^{-1}cm^{-2}$	0.01–45	V_g: 2–3 V	NR		
Carbon nanomaterials									
Graphene-FET	Glucose	GOD	100	~1 μA/mM (est.)	<10	V_{ds}: 0.1 V V_g: 0 V	<200 s (est.)	Buffer: PBS (10 mM) Working pH: 7.2	Glutamate was detected using sensor with GluD
OTFT	Glucose	Graphene-Chitosan-GOD	0.01	370 mV/dec	0.01–1μM	V_g: 0.4 V V_{ds}: 0.05 V	~500 s	Buffer: PBS Working pH: 7.4	Investigated effect of interfere of UA and AA
Graphene-FET	Glucose	Silk fibroin-GOD	100	2.5 μA/mM	0.1–10	V_g: 0 V V_{ds}:0.1 V	~100 s	Buffer: PBS (10 mM) Working pH: 7.4	Stable for 10 mo at room temperat
FET	H_2O_2 & Glucose	Graphene-Chitosan-PtNPs-GOD	0.03	91.7 mV/dec	30 nM–1 mM	V_g: 0.7 V V_{ds}: 0.05 V	~100 s (est.)	Buffer: PBS Working pH: 7.2	No interference observed from and UA
rGO-FET	H_2O_2	MoS_2	1 pM	0.46%/dec	1 pM–100 nM	V_g: 0.1 V V_{ds}: 0.01 V	~1 s	Buffer: PBS Working pH: 7.4	HeLa Cells

FET	H_2O_2	Graphene-Cyt-c	0.1 pM	14%/dec	0.1–100 pM	V_g: 1.75 V V_{ds}: 0.001 V	<1 s	Buffer: PBS Working pH: 7.4	No interference f UA, AA, dopam and glutamate
Others									
SiO_2-MOSC	Glucose	HRP-GOD	5000	1.76 nA/cm^{2}M	<2 M	V_g: 5 V	1200	Dry sensor so no need for a buffer solution	-
Polysilicon wire-ISFET	H_2O_2 & Glucose	APTES-SiNPs-UV treatment	32 pM	12 AmM^{-1}cm^{-2}	10^{-10}–10^{-3} M	V_{ds}: 5 V	NR	Tested solution volume: 0.03 pL (Dry sensor)	Serum

References

1. Chen, S.; Yuan, R.; Chai, Y.; Hu, F. Electrochemical sensing of hydrogen peroxide using metal nanoparticles: A review. Mi-crochim. Acta 2013, 180, 15–32, doi:10.1007/s00604-012-0904-4.
2. Giorgio, M.; Trinei, M.; Migliaccio, E.; Pelicci, P.G. Hydrogen peroxide: A metabolic by-product or a common mediator of ageing signals? Nat. Rev. Mol. Cell Biol. 2007, 8, 722–728, doi:10.1038/nrm2240.
3. Miller, E.W.; Dickinson, B.C.; Chang, C.J. Aquaporin-3 mediates hydrogen peroxide uptake to regulate downstream intr acel-lular signaling. Proc. Natl. Acad. Sci. USA 2010, 107, 15681–15686, doi:10.1073/pnas.1005776107.
4. Sies, H. Hydrogen peroxide as a central redox signaling molecule in physiological oxidative stress: Oxidative eustress. Redox Biol. 2017, 11, 613–619, doi:10.1016/j.redox.2016.12.035.
5. Pi, J.; Bai, Y.; Zhang, Q.; Wong, V.; Floering, L.M.; Daniel, K.; Reece, J.M.; Deeney, J.T.; Andersen, M.E.; Corkey, B.E.; et al. Reactive Oxygen Species as a Signal in Glucose-Stimulated Insulin Secretion. Diabetes 2007, 56, 1783–1791, d oi:10.2337/db06-1601.
6. Liou, G.Y.; Storz, P. Reactive oxygen species in cancer. Free Radic. Res. 2010, 44, 479–496, doi:10.3109/1071576100 3667554.
7. Barnham, K.J.; Masters, C.L.; Bush, A.I. Neurodegenerative diseases and oxidatives stress. Nat. Rev. Drug Discov. 20 04, 3, 205–214, doi:10.1038/nrd1330.
8. Rao, A.V.; Balachandran, B. Role of Oxidative Stress and Antioxidants in Neurodegenerative Diseases. Nutr. Neurosci. 2002, 5, 291–309, doi:10.1080/1028415021000033767.
9. Schöning, M.J.; Poghossian, A. Recent advances in biologically sensitive field-effect transistors (BioFETs). Analyst 200 2, 127, 1137–1151, doi:10.1039/b204444g.
10. Andersen, B.M.; Rasch, M.; Hochlin, K.; Jensen, F.H.; Wismar, P.; Fredriksen, J.E. Decontamination of rooms, medical equip-ment and ambulances using an aerosol of hydrogen peroxide disinfectant. J. Hosp. Infect. 2006, 62, 149–155, d oi:10.1016/j.jhin.2005.07.020.
11. Burmistrova, N.A.; Kolontaeva, O.A.; Duerkop, A. New Nanomaterials and Luminescent Optical Sensors for Detection o f Hydrogen Peroxide. Chemosensors 2015, 3, 253–273, doi:10.3390/chemosensors3040253.
12. Guo, H.; Aleyasin, H.; Dickinson, B.C.; Haskew-Layton, R.E.; Ratan, R.R. Recent advances in hydrogen peroxide imagi ng for biological applications. Cell Biosci. 2014, 4, 1–10, doi:10.1186/2045-3701-4-64.
13. Chen, W.; Cai, S.; Ren, Q.Q.; Wen, W.; Zhao, Y.D. Recent advances in electrochemical sensing for hydrogen peroxide: A re-view. Analyst 2012, 137, 49–58, doi:10.1039/c1an15738h.
14. Liu, H.; Weng, L.; Yang, C. A review on nanomaterial-based electrochemical sensors for H2O2, H2S and NO inside cell s or released by cells. Microchim. Acta 2017, 184, 1267–1283, doi:10.1007/s00604-017-2179-2.
15. Shamkhalichenar, H.; Choi, J.-W. Review—Non-Enzymatic Hydrogen Peroxide Electrochemical Sensors Based on Red uced Graphene Oxide. J. Electrochem. Soc. 2020, 167, 037531, doi:10.1149/1945-7111/ab644a.
16. Aziz, A.; Asif, M.; Ashraf, G.; Azeem, M.; Majeed, I.; Ajmal, M.; Wang, J.; Liu, H. Advancements in electrochemical sensi ng of hydrogen peroxide, glucose and dopamine by using 2D nanoarchitectures of layered double hydroxides or metal

dichalco-genides. A review. Microchim. Acta 2019, 186, 671, doi:10.1007/s00604-019-3776-z.

17. Chen, L.; Compton, R.G. Reference Electrodes for Electrochemical Sensors Based on Redox Couples Immobilized wit hin Nafion Films. ACS Sens. 2019, 4, 1716–1723, doi:10.1021/acssensors.9b00693.
18. Aydoğdu, G.; Zeybek, D.K.; Pekyardımcı, Şule; Kilic, E. A novel amperometric biosensor based on ZnO nanoparti-cles-modified carbon paste electrode for determination of glucose in human serum. Artif. Cells Nanomed. Biotechnol. 2013, 41, 332–338, doi:10.3109/21691401.2012.744994.
19. Soylemez, S.; Yoon, B.; Toppare, L.; Swager, T.M. Quaternized Polymer–Single-Walled Carbon Nanotube Scaffolds for a Chemiresistive Glucose Sensor. ACS Sens. 2017, 2, 1123–1127, doi:10.1021/acssensors.7b00323.
20. Song, E.; Choi, J.W. A selective hydrogen peroxide sensor based on chemiresistive polyaniline nanowires modified with silver catalytic nanoparticles. J. Micromechanics Microengineering 2014, 24, 24, doi:10.1088/0960-1317/24/6/065004.
21. Li, L.; Guo, W.; Lin, Y.; Tang, D.; Liu, J. Facile and feasible conductometric immunoanalytical assay for alpha-fetoprotei n us-ing platinum-functionalized graphitic carbon nitride nanosheets. Anal. Methods 2018, 10, 4886–4893, doi:10.1039/c8ay01789a.
22. Valencia, G.A.; De Oliveira Vercik, L.C.; Vercik, A. A new conductometric biosensor based on horseradish peroxidase i mmo-bilized on chitosan and chitosan/gold nanoparticle films. J. Polym. Eng. 2014, 34, 633–638, doi:10.1515/polyeng-2014-0072.
23. Nouira, W.; Maaref, A.; Elaissari, H.; Vocanson, F.; Siadat, M.; Jaffrezic-Renault, N. Comparative study of conductometr ic glucose biosensor based on gold and on magnetic nanoparticles. Mater. Sci. Eng. C 2013, 33, 298–303, doi:10.1016/j.msec.2012.08.043.
24. Lee, S.H.; Kim, K.H.; Seo, S.E.; Kim, M.I.; Park, S.J.; Kwon, O.S. Cytochrome C-decorated graphene field-effect transi stor for highly sensitive hydrogen peroxide detection. J. Ind. Eng. Chem. 2020, 83, 29–34, doi:10.1016/j.jiec.2019.11.009.
25. Zheng, C.; Jin, X.; Li, Y.; Mei, J.; Sun, Y.; Xiao, M.; Zhang, H.; Zhang, Z.; Zhang, G.J. Sensitive Molybdenum Disulfide Based Field Effect Transistor Sensor for Real-time Monitoring of Hydrogen Peroxide. Sci. Rep. 2019, 9, 1–9, doi:10.1038/s41598-018-36752-y.
26. Shan, J.; Li, J.; Chu, X.; Xu, M.; Jin, F.; Wang, X.; Ma, L.; Fang, X.; Wei, Z.; Wang, X. High sensitivity glucose detection at ex-tremely low concentrations using a MoS2-based field-effect transistor. RSC Adv. 2018, 8, 7942–7948, doi:10.1039/c7ra13614e.
27. Sugiyasu, K.; Swager, T.M. Conducting-Polymer-Based Chemical Sensors: Transduction Mechanisms. Bull. Chem. Soc. Jpn. 2007, 80, 2074–2083, doi:10.1246/bcsj.80.2074.
28. Pundir, C.S.; Deswal, R.; Narwal, V. Quantitative analysis of hydrogen peroxide with special emphasis on biosensors. Bio-process Biosyst. Eng. 2018, 41, 313–329, doi:10.1007/s00449-017-1878-8.
29. Zhang, R.; Chen, W. Recent advances in graphene-based nanomaterials for fabricating electrochemical hydrogen peroxide sensors. Biosens. Bioelectron. 2017, 89, 249–268, doi:10.1016/j.bios.2016.01.080.
30. Olenin, A.Y. Methods of nonenzymatic determination of hydrogen peroxide and related reactive oxygen species. J. Anal. Chem. 2017, 72, 243–255, doi:10.1134/S1061934817030108.
31. Thatikayala, D.; Ponnamma, D.; Sadasivuni, K.K.; Cabibihan, J.J.; Al-Ali, A.K.; Malik, R.A.; Min, B. Progress of Advanced Nanomaterials in the Non-Enzymatic Electrochemical Sensing of Glucose and H2O2. Biosensors 2020, 10, 151, doi:10.3390/bios10110151.
32. Koo, W.-T.; Jang, J.-S.; Kim, I.-D. Metal-Organic Frameworks for Chemiresistive Sensors. Chem 2019, 5, 1938–1963, doi:10.1016/j.chempr.2019.04.013.
33. Kruse, P. Review on water quality sensors. J. Phys. D Appl. Phys. 2018, 51, 203002, doi:10.1088/1361-6463/aabb93.
34. Moonoosawmy, K.R.; Kruse, P. Cause and Consequence of Carbon Nanotube Doping in Water and Aqueous Media. J. Am. Chem. Soc. 2010, 132, 1572–1577, doi:10.1021/ja906820n.
35. Fennell, J.F.; Liu, S.F.; Azzarelli, J.M.; Weis, J.G.; Rochat, S.; Mirica, K.A.; Ravnsbaek, J.B.; Swager, T.M. Nanowire Chemi-cal/Biological Sensors: Status and a Roadmap for the Future. Angew. Chem. Int. Ed. 2016, 55, 1266–1281, doi:10.1002/anie.201505308.
36. Tang, R.; Shi, Y.; Hou, Z.; Wei, L. Carbon Nanotube-Based Chemiresistive Sensors. Sensors (Switzerland) 2017, 17, 882, doi:10.3390/s17040882.
37. Lange, U.; Mirsky, V.M. Chemiresistors based on conducting polymers: A review on measurement techniques. Anal. Chim. Acta 2011, 687, 105–113, doi:10.1016/j.aca.2010.11.030.
38. Jaffrezic-Renault, N.; Dzyadevych, S.V. Conductometric Microbiosensors for Environmental Monitoring. Sensors 2008, 8, 2569–2588, doi:10.3390/s8042569.
39. Watson, L.D.; Maynard, P.; Cullen, D.C.; Sethi, R.S.; Brettle, J.; Lowe, C.R. A microelectronic conductimetric biosensor. Top. Catal. 1987, 3, 101–115, doi:10.1016/s0265-928x(87)80003-2.
40. Hwa-Il, S.; Chang-Soo, K.; Byung-Ki, S.; Terence, Y.; Son Mun-Tak, H.M. ISFET glucose sensor based on a new principle using the electrolysis of hydrogen peroixde. Sens. Actuators B Chem. 1997, 40, 1–5.

41. Shul'Ga, A.A.; Gibson, T.D. An alternative microbiosensor for hydrogen peroxide based on an enzyme field effect transi stor with a fast response. Anal. Chim. Acta 1994, 296, 163–170, doi:10.1016/0003-2670(94)80260-2.

42. Sohn, B.-K.; Cho, B.-W.; Kim, C.-S.; Kwon, D.-H. ISFET glucose and sucrose sensors by using platinum electrode and pho-to-crosslinkable polymers. Sens. Actuators B Chem. 1997, 41, 7–11, doi:10.1016/s0925-4005(97)80271-7.

43. Sergeyeva, T.A.; Lavrik, N.V.; Rachkov, A.E.; Kazantseva, Z.I.; Piletsky, S.A.; El'Skaya, A.V. Hydrogen peroxide—Sensi tive enzyme sensor based on phthalocyanine thin film. Anal. Chim. Acta 1999, 391, 289–297, doi:10.1016/s0003-2670 (99)00203-2.

44. Dam, V.-A.T.; Oithuis, W.; Bergveld, P.; Berg, A.ven den. Catalytic Hydrogen Peroxide decompositon on pervoskite oxid e. The 13th International Conference on Solid-State Sensors, Actuators and Microsystems, 2005. Digest of Technical P apers. TRANSDUCERS '05., Seoul, South Korea, 2005, pp. 1840-1843 Vol. 2, doi: 10.1109/SENSOR.2005.1497453.

45. Kim, C.S.; Seo, H. Il; Lee, C.H.; Sohn, B.K. Miniaturized ISFET glucose sensor including a new structure actuation syst em. In Proceedings of the International Solid State Sensors and Actuators Conference (Transducers '97), Chicago, IL, USA, 19 June 1997; Volume 2, pp. 911–914, doi:10.1109/sensor.1997.635250.

46. Diallo, A.K.; Djeghlaf, L.; Mazenq, L.; Launay, J.; Sant, W.; Temple-Boyer, P. Development of pH-based ElecFET biosen sors for lactate ion detection. Biosens. Bioelectron. 2013, 40, 291–296, doi:10.1016/j.bios.2012.07.063.

47. Van Der Spiegel, J.; Lauks, I.; Chan, P.; Babic, D. The extended gate chemically sensitive field effect transistor as multi -species microprobe. Sens. Actuators 1983, 4, 291–298, doi:10.1016/0250-6874(83)85035-5.

48. Teh, K.-S.; Lin, L. MEMS sensor material based on polypyrrole–carbon nanotube nanocomposite: Film deposition and c har-acterization. J. Micromechanics Microengineering 2005, 15, 2019–2027, doi:10.1088/0960-1317/15/11/005.

49. Salila Vijayalal Mohan, H.K.; Hansen Varghese, R.; Wong, C.H.; Zheng, L.; Yang, J. Epigallocatechin gallate decorated carbon nanotube chemiresistors for ultrasensitive glucose detection. Org. Electron. 2016, 28, 210–216, doi:10.1016/j.or gel.2015.10.032.

50. Song, E.; Da Costa, T.H.; Choi, J.W. A chemiresistive glucose sensor fabricated by inkjet printing. Microsyst. Technol. 2 017, 23, 3505–3511, doi:10.1007/s00542-016-3160-4.

51. Song, E.; Tortorich, R.P.; Da Costa, T.H.; Choi, J.W. Inkjet printing of conductive polymer nanowire network on flexible s ub-strates and its application in chemical sensing. Microelectron. Eng. 2015, 145, 143–148, doi:10.1016/j.mee.2015.0 4.004.

52. Song, E.; Choi, J.W. Multi-analyte detection of chemical species using a conducting polymer nanowire-based sensor ar ray platform. Sens. Actuators B Chem. 2015, 215, 99–106, doi:10.1016/j.snb.2015.03.039.

53. Ansari, S.G.; Ansari, Z.A.; Wahab, R.; Kim, Y.S.; Khang, G.; Shin, H.S. Glucose sensor based on nano-baskets of tin ox ide templated in porous alumina by plasma enhanced CVD. Biosens. Bioelectron. 2008, 23, 1838–1842, doi:10.1016/j. bios.2008.02.022.

54. Hnaien, M.; Lagarde, F.; Jaffrezic-Renault, N. A rapid and sensitive alcohol oxidase/catalase conductometric biosensor for alcohol determination. Talanta 2010, 81, 222–227, doi:10.1016/j.talanta.2009.11.061.

55. Bouyahia, N.; Hamlaoui, M.L.; Hnaien, M.; Lagarde, F.; Jaffrezic-Renault, N. Impedance spectroscopy and conductome tric biosensing for probing catalase reaction with cyanide as ligand and inhibitor. Bioelectrochemistry 2011, 80, 155–16 1, doi:10.1016/j.bioelechem.2010.07.006.

56. Nguyen-Boisse, T.T.; Saulnier, J.; Jaffrezic-Renault, N.; Lagarde, F. Highly sensitive conductometric biosensors for total lactate, d- and l-lactate determination in dairy products. Sens. Actuators B Chem. 2013, 179, 232–239, doi:10.1016/j.sn b.2012.10.021.

57. Liu, H.; Yang, Y.; Chen, P.; Zhong, Z. Enhanced conductometric immunoassay for hepatitis B surface antigen using dou -ble-codified nanogold particles as labels. Biochem. Eng. J. 2009, 45, 107–112, doi:10.1016/j.bej.2009.03.002.

58. Mahadeva, S.K.; Kim, J. Conductometric glucose biosensor made with cellulose and tin oxide hybrid nanocomposite. S ens. Actuators B Chem. 2011, 157, 177–182, doi:10.1016/j.snb.2011.03.046.

59. Volotovsky, V.; Kim, N. Cyanide determination by an ISFET-based peroxidase biosensor. Biosens. Bioelectron. 1998, 1 3, 1029–1033, doi:10.1016/s0956-5663(98)00004-9.

60. Forzani, E.S.; Zhang, H.; Nagahara, L.A.; Amlani, I.; Tsui, R.; Tao, N. A Conducting Polymer Nanojunction Sensor for Gl u-cose Detection. Nano Lett. 2004, 4, 1785–1788, doi:10.1021/nl049080l.

61. Luo, X.L.; Xu, J.J.; Zhao, W.; Chen, H.Y. A novel glucose ENFET based on the special reactivity of MnO2 nanoparticle s. Bio-sens. Bioelectron. 2004, 19, 1295–1300, doi:10.1016/j.bios.2003.11.019.

62. Bernards, D.A.; Macaya, D.J.; Nikolou, M.; DeFranco, J.A.; Takamatsu, S.; Malliaras, G.G. Enzymatic sensing with org anic electrochemical transistors. J. Mater. Chem. 2008, 18, 116–120, doi:10.1039/b713122d.

63. Liu, J.; Agarwal, M.; Varahramyan, K. Glucose sensor based on organic thin film transistor using glucose oxidase and c on-ducting polymer. Sens. Actuators B Chem. 2008, 135, 195–199, doi:10.1016/j.snb.2008.08.009.

64. Yoon, H.; Ko, S.; Jang, J. Field-Effect-Transistor Sensor Based on Enzyme-Functionalized Polypyrrole Nanotubes for G lucose Detection. J. Phys. Chem. B 2008, 112, 9992–9997, doi:10.1021/jp800567h.

65. Park, J.W.; Park, S.J.; Kwon, O.S.; Lee, C.; Jang, J. Polypyrrole Nanotube Embedded Reduced Graphene Oxide Transducer for Field-Effect Transistor-Type H2O2 Biosensor. Anal. Chem. 2014, 86, 1822–1828, doi:10.1021/ac403770x.
66. Park, J.W.; Lee, C.; Jang, J. High-performance field-effect transistor-type glucose biosensor based on nanohybrids of carbox-ylated polypyrrole nanotube wrapped graphene sheet transducer. Sens. Actuators B Chem. 2015, 208, 532–537, doi:10.1016/j.snb.2014.11.085.
67. Yin, L.T.; Chou, J.C.; Chung, W.Y.; Sun, T.P.; Hsiung, K.P.; Hsiung, S.K. Glucose ENFET doped with MnO2 powder. Sens. Actuators B Chem. 2001, 76, 187–192, doi:10.1016/s0925-4005(01)00629-3.
68. Anh, D.T.V.; Olthuis, W.; Bergveld, P. Electroactive gate materials for a hydrogen peroxide sensitive eMOSFET. IEEE Sens. J. 2002, 2, 26–33, doi:10.1109/7361.987058.
69. Lin, J.J.; Wu, Y.L.; Hsu, P.Y. Novel Dry-Type Glucose Sensor Based on a Metal–Oxide–Semiconductor Capacitor Structure with Horseradish Peroxidase + Glucose Oxidase Catalyzing Layer. Jpn. J. Appl. Phys. Part 1 Regul. Pap. Short Notes Rev. Pap. 2007, 46, 6871–6874, doi:10.1143/jjap.46.6871.
70. Ozasa, K.; Nemoto, S.; Li, Y.; Hara, M.; Maeda, M.; Mochitate, K. Contact angle and biocompatibility of sol-gel prepared TiO2 thin films for their use as semiconductor-based cell-viability sensors. Surf. Interface Anal. 2008, 40, 579–583, doi:10.1002/sia.2729.
71. Chen, Y.; Lee, Y.D.; Vedala, H.; Allen, B.L.; Star, A. Exploring the Chemical Sensitivity of a Carbon Nanotube/Green Tea Composite. ACS Nano 2010, 4, 6854–6862, doi:10.1021/nn100988t.
72. Wu, Y.L.; Hsu, P.Y.; Lin, J.J. Polysilicon wire glucose sensor highly immune to interference. Biosens. Bioelectron. 2011, 26, 2281–2286, doi:10.1016/j.bios.2010.09.052.
73. Ahmad, R.; Tripathy, N.; Park, J.H.; Hahn, Y.B. A comprehensive biosensor integrated with a ZnO nanorod FET array for selective detection of glucose, cholesterol and urea. Chem. Commun. 2015, 51, 11968–11971, doi:10.1039/c5cc03656a.
74. Bartlett, P.N.; Birkin, P.R.; Wang, J.H.; Palmisano, F.; De Benedetto, G. An Enzyme Switch Employing Direct Electrochemical Communication between Horseradish Peroxidase and a Poly(aniline) Film. Anal. Chem. 1998, 70, 3685–3694, doi:10.1021/ac971088a.
75. Raffa, D.; Leung, K.T.; Battaglini, F. A Microelectrochemical Enzyme Transistor Based on an N-Alkylated Poly(Aniline) and Its Application to Determine Hydrogen Peroxide at Neutral pH. Anal. Chem. 2003, 75, 4983–4987, doi:10.1021/ac0341620.
76. Huang, Y.; Dong, X.; Shi, Y.; Li, C.M.; Li, L.J.; Chen, P. Nanoelectronic biosensors based on CVD grown graphene. Nanoscale 2010, 2, 1485–1488, doi:10.1039/c0nr00142b.
77. Kwak, Y.H.; Choi, D.S.; Kim, Y.N.; Kim, H.; Yoon, D.H.; Ahn, S.S.; Yang, J.W.; Yang, W.S.; Seo, S. Flexible glucose sensor using CVD-grown graphene-based field effect transistor. Biosens. Bioelectron. 2012, 37, 82–87, doi:10.1016/j.bios.2012.04.042.
78. You, X.; Pak, J.J. Graphene-based field effect transistor enzymatic glucose biosensor using silk protein for enzyme immobiliza-tion and device substrate. Sens. Actuators B Chem. 2014, 202, 1357–1365, doi:10.1016/j.snb.2014.04.079.
79. Zhu, Z.; Mabeck, J.T.; Zhu, C.; Cady, N.C.; Batt, A.; Malliaras, G.G. A simple PEDOT:PSS transistor for glucose sensing at neutral pH. Chem. Commun. 2004, 13, 1556–1557.
80. Kim, Y.; Do, J.; Kim, J.; Yang, S.Y.; Malliaras, G.G.; Ober, C.K.; Kim, E. A Glucose Sensor Based on an Organic Electrochemi-cal Transistor Structure Using a Vapor Polymerized Poly(3,4-ethylenedioxythiophene) Layer. Jpn. J. Appl. Phys. 2010, 49, doi:10.1143/jjap.49.01ae10.
81. Liao, J.; Lin, S.; Yang, Y.; Liu, K.; Du, W. Highly selective and sensitive glucose sensors based on organic electrochemical transistors using TiO2 nanotube arrays-based gate electrodes. Sens. Actuators B Chem. 2015, 208, 457–463, doi:10.1016/j.snb.2014.11.038.
82. Welch, M.E.; Doublet, T.; Bernard, C.; Malliaras, G.G.; Ober, C.K. A glucose sensor via stable immobilization of the GOx en-zyme on an organic transistor using a polymer brush. J. Polym. Sci. Part A Polym. Chem. 2015, 53, 372–377, doi:10.1002/pola.27392.
83. Jung, D.-U.-J.; Ahmad, R.; Hahn, Y.B. Nonenzymatic flexible field-effect transistor based glucose sensor fabricated using NiO quantum dots modified ZnO nanorods. J. Colloid Interface Sci. 2018, 512, 21–28, doi:10.1016/j.jcis.2017.10.037.
84. Liao, C.; Zhang, M.; Niu, L.; Zheng, Z.; Yan, F. Highly selective and sensitive glucose sensors based on organic electrochemical transistors with graphene-modified gate electrodes. J. Mater. Chem. B 2013, 1, 3820–3829, doi:10.1039/c3tb20451k.
85. Zhang, M.; Liao, C.; Mak, C.H.; You, P.; Mak, C.L.; Yan, F. Highly sensitive glucose sensors based on enzyme-modified whole-graphene solution-gated transistors. Sci. Rep. 2015, 5, 1–6, doi:10.1038/srep08311.